

Mainz preprint
July 1994
October 1994 (rev.)

Correlation Function at β_t in the Disordered Phase of 2D Potts Models

Wolfhard Janke and Stefan Kappler

Institut für Physik, Johannes Gutenberg-Universität Mainz
Staudinger Weg 7, 55099 Mainz, Germany

Abstract

We use Monte Carlo simulations to measure the spin-spin correlation function in the disordered phase of two-dimensional q -state Potts models with $q = 10, 15$, and 20 at the first-order transition point β_t . To extract the correlation length ξ_d from the exponential decay of the correlation function over several decades with the desired accuracy we make extensively use of cluster-update techniques and improved estimators. Our results for ξ_d are compatible with an analytic formula. As a byproduct we also measure the energy moments in the disordered phase and find very good agreement with a recent large q expansion at β_t .

1 Introduction

An important quantity to characterize the properties of a statistical system is the correlation length ξ which can be extracted from the exponential decay of a correlation function $G(x)$ in the limit of large distances x . Usually various definitions of $G(x)$ are possible and it is a priori unclear which one is best suited in numerical Monte Carlo simulations. There are only very few models for which the correlation length is exactly known and can thus serve as a testing ground for the employed numerical techniques. The best known example is the two-dimensional Ising model where the correlation length is exactly known at all temperatures in both the high- and low-temperature phase [1]. Only quite recently also for two-dimensional q -state Potts models on simple square lattices an analytic formula for the correlation length could be derived [2, 3]. Here, however, the correlation length is only known at one special temperature, namely at the first-order transition point β_t of this model for $q \geq 5$. More precisely, by comparing with a large q expansion, it could be argued [4] that the analytic result in Ref.[2] refers to the correlation length $\xi_d(\beta_t)$ in the disordered phase.

Using exact duality arguments and the (weak) assumption of complete wetting (which can only be proven in the limit of large q) this result was then converted into an explicit expression for the order-disorder interface tension, $\sigma_{od} = 1/2\xi_d$ [4]. This formula turned out to be in good agreement with previous (and thus completely unbiased) numerical interface-tension data for $q = 7$ [5] and $q = 10$ [6], and also subsequent high-precision studies obtained compatible values [7]. The purpose of this note is to present direct numerical tests of the formula for $\xi_d(\beta_t)$.

2 The model and observables

The two-dimensional q -state Potts model is defined by the partition function [8]

$$Z = \sum_{\{s_i\}} e^{-\beta E}; \quad E = - \sum_{\langle ij \rangle} \delta_{s_i s_j}; \quad s_i = 1, \dots, q, \quad (1)$$

where $i = (i_x, i_y)$ denote the lattice sites of a square lattice of size $V = L_x \times L_y$, $\langle ij \rangle$ are nearest-neighbor pairs and $\delta_{s_i s_j}$ is the Kronecker delta symbol. In the infinite volume limit this model exhibits on simple square

lattices for $q \leq 4$ ($q \geq 5$) a 2nd (1st) order phase transition at $\beta_t = \ln(1 + \sqrt{q})$. At β_t also the internal energy densities e_o and e_d of the ordered and disordered phase are known exactly while for the corresponding specific heats only the difference $\Delta c = c_d - c_o$ could be derived analytically.

In the disordered phase the spin-spin correlation function can be defined as

$$G(i, j) \equiv \langle \delta_{s_i s_j} - \frac{1}{q} \rangle. \quad (2)$$

For numerical purposes it is more convenient to consider the $k_y = 0$ projection of G ,

$$g(i_x, j_x) = \frac{1}{L_y} \sum_{i_y, j_y} G(i, j), \quad (3)$$

which should be free of power-like prefactors in the large-distance behaviour. For periodic boundary conditions translational invariance implies that g depends only on $|i_x - j_x|$, and for convenience we shall sometimes simply write $g(x)$. A useful test of the consistency of our data is provided by the magnetic susceptibility

$$\chi = \frac{1}{V(q-1)} \langle [\sum_i (q\delta_{s_i,1} - 1)]^2 \rangle, \quad (4)$$

which can be computed from the area under the correlation function,

$$\chi = \frac{q}{V(q-1)} \sum_{i,j} G(i, j) = \frac{q}{q-1} \sum_{i_x=1}^{L_x} g(i_x, 0). \quad (5)$$

3 The simulation

In our Monte Carlo study we investigated the correlation function in the disordered phase at β_t for $q = 10, 15$ and 20 on lattices of size $V = L \times L$ and $V = 2L \times L$ with $L = 150, 60$ and 40 ($\approx 14\xi_d$). To take advantage of translational invariance we used periodic boundary conditions but chose the lattice sizes large enough to suppress tunneling events. This guaranteed that, starting from a completely random configuration, the system remained a sufficiently long time in the disordered phase to perform statistically meaningful measurements. Since in this situation it is not obvious which update algorithm performs best we first performed for the $L \times L$ lattices a quite elaborate efficiency study of the most popular update algorithms, the local

Metropolis and heat-bath algorithms and the non-local Wolff single-cluster [9] and Swendsen-Wang multiple-cluster [10] algorithms. By measuring the integrated autocorrelation times $\tau_{\text{int},e}$ of the energy it became immediately clear that the Metropolis algorithm is not a good candidate; see Table 1. Also the multiple-cluster algorithm seems to be inferior in this application. The other two algorithms, on the other hand, exhibit comparable $\tau_{\text{int},e}$, in particular for large q where the average cluster size is small. Taking into account the details of our implementation, this makes it difficult to decide between the two alternatives on the basis of $\tau_{\text{int},e}$ alone. Being mainly interested in the long-distance behaviour of correlation functions we therefore also looked at the integrated autocorrelation times $\tau_{\text{int},g(x)}$ of these quantities. Our results for $q = 20$ are shown in Fig. 1. As expected we find that for the local heat-bath algorithm the autocorrelations grow with distance, while for the non-local single-cluster algorithm they decrease. On the basis of these tests we finally decided to use the single-cluster algorithm for all production runs. It should be mentioned that for any algorithm we used the multiple-cluster decomposition of a given spin configuration for measurements using the improved estimator

$$G(i, j) = \frac{q-1}{q} \langle \Theta(i, j) \rangle, \quad (6)$$

where $\Theta(i, j) = 1$, if i and j belong to the same cluster, and $\Theta = 0$ otherwise. By performing the summations in eq.(3) one easily derives an improved estimator for $g(i_x, 0)$.

In the production runs we updated the spins after many single-cluster iterations with one multiple-cluster step to facilitate the most efficient use of the “improved estimator” (6). In units of $\tau_{\text{int},e}$ the run time on the $L \times L$ ($2L \times L$) lattices was about 35 000 (60 000) for $q = 10$, 116 000 (230 000) for $q = 15$, and 72 000 (35 000) for $q = 20$. All error bars are estimated by means of the jack-knife technique [11]. Finally it is worth mentioning that all our correlation function data are stored in such a way that they can be reweighted to nearby temperatures in both directions; in this way we have also computed extrapolations of the correlation length into the metastable disordered region [12].

4 Results

4.1 Energy moments

To convince ourselves that the system was always in the disordered phase, we monitored the time series of the energy measurements and computed the first three moments of the energy distribution, $e_d \equiv \langle E \rangle / V$, $c_d = \beta_t^2 \mu_d^{(2)} \equiv \beta_t^2 (\langle E^2 \rangle - \langle E \rangle^2) / V$, and $\mu_d^{(3)} = \langle (E - \langle E \rangle)^3 \rangle / V$. While e_d can be compared with exact results, c_d and $\mu_d^{(3)}$ can be related by duality to the corresponding moments in the ordered phase,

$$c_d = c_o + \beta_t^2 (e_d - e_o) / \sqrt{q}, \quad (7)$$

$$\mu_d^{(3)} = -\mu_o^{(3)} + 2(1 - q) / q^{3/2} + 3(e_d - e_o) / q + 6c_o / \beta_t^2 \sqrt{q}, \quad (8)$$

which have recently been estimated by means of Padé extrapolations of large q series expansions [13]. Our Monte Carlo estimates for the $L \times L$ and $2L \times L$ lattices can be found in Table 2, together with the Padé extrapolations as given in the reanalysis of Ref.[14] (using series expansions extended by one term), which are practically indistinguishable from our own Padé analysis. A comparison of the two sets of numbers shows excellent agreement between the two methods, even for the third moment and small q .

Estimates of c_d from the finite-size scaling behaviour of the specific-heat maxima gave a consistent value of 6.0(2) [15] for $q = 20$, but much too small values for $q = 10$ [16, 17], while recent estimates from very long high-temperature series expansions [18] are too large by a factor of about 2. Only finite-size scaling *at* the transition point β_t seems to give sensible results, at least for $q = 10$ [17].

4.2 Susceptibility

As a further test of the consistency of our data we compared the magnetic susceptibility computed according to eq.(5) with measurements using the improved cluster estimators

$$\chi = \langle |C| \rangle_{SC} = \langle |C|^2 \rangle_{SW} / \langle |C| \rangle_{SW}, \quad (9)$$

where $\langle \cdot \rangle_{SC}$ ($\langle \cdot \rangle_{SW}$) refers to the average taken from the single (multiple) cluster update. As is shown in Table 3, in all cases we obtained excellent agreement between the three estimators.

4.3 Correlation function

Let us now turn to the main subject of this note, the correlation function. A preliminary report of a first set of $L \times L$ data was recently given in Ref.[19]. Our complete set of measurements now consists of data for G along the coordinate axes and for the projected correlation functions $g(x)$ for $q = 10, 15$, and 20 on $L \times L$ and $2L \times L$ lattices with $L = 150, 60$ and 40 . The average of the $k_y = 0$ and $k_x = 0$ projections on the $L \times L$ lattices and the $k_y = 0$ projection on the $2L \times L$ lattices, i.e. $g(x)$, are shown in the semi-log plots of Fig. 2. The quite pronounced curvature for small x indicates that the simplest two-parameter Ansatz for periodic boundary conditions,

$$g(x) = a \operatorname{ch}\left(\frac{L/2 - x}{\xi_d}\right), \quad (10)$$

which takes into account only the lowest excitation (largest correlation length), can only be justified for very large x . We have therefore considered also the more general Ansatz

$$g(x) = a \operatorname{ch}\left(\frac{L/2 - x}{\xi_d}\right) + b \operatorname{ch}\left(c \frac{L/2 - x}{\xi_d}\right), \quad (11)$$

with four parameters a, b, c , and ξ_d .

Since non-linear four-parameter fits are notoriously difficult to control, we first fixed ξ_d at its theoretical value ($\xi_d = 10.559519\dots, 4.180954\dots$, and $2.695502\dots$ for $q = 10, 15$, and 20 , respectively), and optimized only the remaining three parameters. The resulting fits to the $L \times L$ and $2L \times L$ data are shown in Fig. 2 as dotted and solid lines, respectively. Over a wide range up to about $x \approx (5 \dots 6)\xi_d$ the lines are excellent interpolations of the data. At very large distances, however, we also see a clear tendency of the fits to lie systematically above the data. This already indicates that unconstrained fits to the Ansatz (11) over the same x range with ξ_d as a *free* parameter should somewhat underestimate the analytical value of ξ_d .

In fact, this is what we observed in the unconstrained fits to both the $L \times L$ and $2L \times L$ data. In order to estimate systematic errors we performed fits to both Ansätze using varying fit intervals. As a general tendency we noticed a trend to higher values for ξ_d when restricting the fit interval to larger x values, but then also the statistical errors grow rapidly. For $q = 10$ this is illustrated in Fig. 3(a), where x_{\min} denotes the smallest x value included in the fits. The

last point used was $x_{\max} = L/2$ for both geometries. For the four-parameter fits we have stopped increasing x_{\min} as soon as the error on the amplitude b became comparable with its central value. For a reasonable range of x_{\min} values satisfying this criterion our results are collected in Table 4. Here we also give the results of fits of $g(y)$, i.e., the $k_x = 0$ projection along the short direction of the $2L \times L$ lattices. The fits of $g(x)$ with the smallest x_{\min} values are shown in Fig. 2 as long ($L \times L$) and short ($2L \times L$) dashed lines. For the parameter c we obtain from the unconstrained four-parameter fits the q independent estimates of $c \approx 1.5 - 2$, with a clear tendency of decreasing c for increasing x_{\min} . This observation is consistent with the constrained three-parameter fits with ξ_d held fixed at its analytical value where we find the quite stable estimate of $c = 1.5 \pm 0.1$, again for all three values of q .

Our numerical estimates for ξ_d underestimate the analytical values by about 10 – 20% for both lattice geometries. The relative deviation clearly increases with increasing q . For some fit ranges we have repeated the analysis using so-called correlated fits [20] which, in general, seemed to be a little more stable. We did not observe, however, any significant increase of the estimates for ξ_d . We also investigated whether the Fourier transforms of g or G are less susceptible to systematic corrections and thus easier to analyze. Unfortunately, the answer is no. In fact, the fitted values of ξ_d turn out to be even smaller than in the corresponding real space fits (if comparable fit intervals are used).

Of course, the problem is that at the distances we have studied so far ($x_{\max} = L/2 \approx 7\xi_d$) even higher excitations cannot be neglected. Due to convexity properties it is then natural that ξ_d is underestimated by using the truncated Ansatz (11). This general trend is illustrated in another way in Fig. 3(b) where we plot for $q = 10$ an effective correlation length defined by the local slopes of $g(x)$,

$$\xi_d^{\text{eff}} = 1/\ln [g(x)/g(x + 1)], \quad (12)$$

as a function of the distance x for both the $L \times L$ as well as the $2L \times L$ data. For large x we expect $\xi_d^{\text{eff}} = \xi_d$. We do observe a clear increase of ξ_d^{eff} , but it is of course still a long way to $\xi_d = 10.56$. In particular with the $L \times L$ data it is difficult to extrapolate to the correct value since the effects of the periodic boundary conditions set in much too early. For the $2L \times L$ data, on the other hand, the three-parameter fit (with ξ_d held fixed at its theoretical

value) indicates how the data should behave for very large distances in the long direction of the lattice. At $x = 100$, however, $g(x)/g(0) \approx 5 \times 10^{-6}$ which is very difficult to measure accurately, even with cluster algorithms and improved observables. In fact, this number reflects how improbable it is to generate a cluster with diameter of about 100 (recall the improved estimator (6)). To cope with this problem we are currently investigating a special type of simulation with a reweighted Hamiltonian designed to increase these probabilities. Using standard simulation techniques it would take an enormous amount of computing time to follow the decay of correlation functions over more than 5 or 6 decades with the necessary accuracy.

As a check of our analysis we put $q = 2$ in our programs, and thus simulated the Ising model in the disordered phase at $\beta = 0.71 \approx 0.80\beta_c$. Here the exactly known correlation length is $\xi_d = 2.728865\dots$ [1], a value that is comparable to $\xi_d(\beta_t)$ of the $q = 20$ Potts model. Our data points for $g(x)$ on $L \times L$ and $2L \times L$ lattices with $L = 40$ shown in Fig. 4 look perfectly straight in a semi-log plot. Consequently, the much simpler fit of the form (10) was sufficient. As a result we obtained from the fits (with $x_{\min} = 1$) shown in Fig. 4 the estimates of $\xi_d = 2.7232(35)$ ($L \times L$) and $\xi_d = 2.7275(24)$ ($2L \times L$), and for a fit in the short direction of the $2L \times L$ lattice $\xi_d = 2.7283(20)$. All these estimates are in very good agreement with the theoretical value, showing that the employed techniques work at least in principle.

5 Discussion

Previous numerical estimates of the correlation length at β_t for $q = 10$ [21, 22, 23] resulted in values of about $\xi \approx 6$ which are much smaller than the theoretical prediction of $\xi_d = 10.56$. The Fernandez *et al.* [22] value of 6.1(5) is obtained from an extrapolation of simulations at $\beta < \beta_t$ and thus definitely refers to the correlation length in the disordered phase. From our experience with correlation function fits and direct tests we believe that their values of ξ_d for $\beta < \beta_t$ are already underestimated. Since the simulation points are relatively far away from β_t , the systematic errors are further enhanced by the extrapolation procedure used in Ref. [22]. The interpretation of the data of Peczak and Landau [21] and Gupta and Irbäck [23] is less clear to us. By repeating the simulations of Ref.[23] we are quite convinced

that their technique yields a weighted average of the ordered and disordered correlation function which is then analyzed to obtain ξ . By using a projection to a momentum $k_1 = 2\pi/L$, the ordered phase is treated properly, but the weighted average makes the final interpretation somewhat unclear. Similarly, since the simulations in Ref.[21] are performed at the specific-heat maximum whose finite-size scaling behaviour is governed by the transitions between the ordered and disordered phase, it is very unlikely that their ξ refers to a pure phase correlation length. In view of these problems it is astonishing that all three methods yield about the same value for ξ . In order to understand this puzzling coincidence we are currently investigating also the correlation length in the ordered phase and first results will be available soon in a separate publication [24].

Constrained fits with $\xi_d(\beta_t)$ held fixed at its theoretical value clearly indicate that our data for the projected correlation function $g(x)$ in the disordered phase at β_t are compatible with the analytical prediction of Refs.[2, 3]. By performing unconstrained fits, however, we cannot really confirm the theoretical values. Rather we systematically underestimate ξ_d by about 10 – 20% in simulations of $L \times L$ as well as $2L \times L$ lattices. We attribute this to higher mass excitations which cannot be neglected at the distances investigated so far. To include these corrections in the fits, however, would require much more precise data. In a comparative study of 2D Ising correlation functions no such problems were encountered and the exact value of the correlation length could be reproduced with high precision.

Acknowledgements

We would like to thank R. Lacaze and A. Morel for interesting discussions on the energy moments and for communicating their unpublished results. WJ gratefully acknowledges a Heisenberg fellowship by the DFG and SK thanks the Graduiertenkolleg “Physik und Chemie supramolekularer Systeme” for financial support. The Monte Carlo simulations were performed on the CRAY Y-MP of the Höchstleistungsrechenzentrum Jülich, the CRAY Y-MP’s of the Norddeutscher Rechnerverbund in Kiel and Berlin, and on the cluster of fast RISC workstations at Mainz.

References

- [1] B.M. Mc Coy and T.T. Wu, *The Two-Dimensional Ising Model* (Harvard University Press, Cambridge, Massachusetts, 1973); C. Itzykson and J.-M. Drouffe, *Statistical Field Theory*, Vol. I, (Cambridge University Press, Cambridge, 1989).
- [2] E. Buffenoir and S. Wallon, *J. Phys.* **A26** (1993) 3045.
- [3] A. Klümper, *Int. J. Mod. Phys.* **B4** (1990) 871; A. Klümper, A. Schadschneider, and J. Zittartz, *Z. Phys.* **B76** (1989) 247.
- [4] C. Borgs and W. Janke, *J. Phys. I (France)* **2** (1992) 2011.
- [5] W. Janke, B.A. Berg, and M. Katoot, *Nucl. Phys.* **B382** (1992) 649.
- [6] B.A. Berg and T. Neuhaus, *Phys. Rev. Lett.* **68** (1992) 9.
- [7] For a table of results and references, see W. Janke, in *IMACS '93* proceedings, St. Louis, *Int. J. Mod. Phys.* **C5** (1994) 75; and Mainz preprint (March 1994), to appear in *Computer Simulations in Condensed Matter Physics VII*, eds. D.P. Landau, K.K. Mon, and H.B. Schüttler (Springer Verlag, Heidelberg, Berlin, 1994).
- [8] F.Y. Wu, *Rev. Mod. Phys.* **54** (1982) 235; **55** (1983) 315(E).
- [9] U. Wolff, *Phys. Rev. Lett.* **62** (1989) 361.
- [10] R.H. Swendsen and J.S. Wang, *Phys. Rev. Lett.* **58** (1987) 86.
- [11] R.G. Miller, *Biometrika* **61** (1974) 1; B. Efron, *The Jackknife, the Bootstrap and other Resampling Plans* (SIAM, Philadelphia, PA, 1982).
- [12] W. Janke and S. Kappler, work in progress.
- [13] T. Bhattacharya, R. Lacaze, and A. Morel, *Europhys. Lett.* **23** (1993) 547; *Nucl. Phys. B (Proc. Suppl.)* **34** (1994) 671.
- [14] T. Bhattacharya, R. Lacaze, and A. Morel, private communication, and to be published.
- [15] A. Billoire, T. Neuhaus, and B.A. Berg, *Nucl. Phys.* **B396** (1993) 779.

- [16] J. Lee and J.M. Kosterlitz, Phys. Rev. **B43** (1991) 3265.
- [17] A. Billoire, R. Lacaze, and A. Morel, Nucl. Phys. **B370** (1992) 773.
- [18] K.M. Briggs, I.G. Enting, and A.J. Guttmann, J. Phys. **A27** (1994) 1503.
- [19] W. Janke and S. Kappler, Nucl. Phys. **B** (Proc. Suppl.) **34** (1994) 674.
- [20] C. Michael, Liverpool preprint LTH 321, hep-lat/9310026 (October 1993); and references therein.
- [21] P. Peczak and D.P. Landau, Phys. Rev. **B39** (1989) 11932.
- [22] L.A. Fernandez, J.J. Ruiz-Lorenzo, M.P. Lombardo, and A. Tarancón, Phys. Lett. **B277** (1992) 485.
- [23] S. Gupta and A. Irbäck, Phys. Lett. **B286** (1992) 112.
- [24] W. Janke and S. Kappler, to be published.

Tables

Table 1: Integrated autocorrelation times of the energy on $L \times L$ lattices at β_t in the disordered phase for different update algorithms in units of sweeps. The results for Wolff's single-cluster update are rescaled to these units.

Algorithm	$q = 10$	$q = 15$	$q = 20$
Metropolis	≈ 2000	400(100)	-
Heatbath	125(25)	19(5)	11(1)
Swendsen-Wang	175(20)	-	67(9)
Wolff	52(7)	23(2)	17(2)

Table 2: Comparison of numerical and analytical results for energy moments at β_t in the disordered phase.

Observable	$q = 10$	$q = 15$	$q = 20$
e_d (MC, $L \times L$)	-0.96812(15)	-0.75053(13)	-0.62648(20)
e_d (MC, $2L \times L$)	-0.968190(81)	-0.750510(65)	-0.626555(97)
e_d (exact)	-0.968203...	-0.750492...	-0.626529...
c_d (MC, $L \times L$)	18.33(17)	8.695(47)	6.144(43)
c_d (MC, $2L \times L$)	18.34(12)	8.665(29)	6.140(27)
c_d (large q)	18.5(1)	8.66(3)	6.133(5)
$\mu_d^{(3)}$ (MC, $L \times L$)	-2010(100)	-171.0(5.1)	-54.7(1.9)
$\mu_d^{(3)}$ (MC, $2L \times L$)	-2031(73)	-176.1(3.8)	-53.9(1.5)
$\mu_d^{(3)}$ (large q)	-1833(40)	-174(4)	-54.6(4)

Table 3: The magnetic susceptibility at β_t in the disordered phase from three different estimators.

Lattice	Observable	$q = 10$	$q = 15$	$q = 20$
$L \times L$	$\frac{q}{q-1} \sum_{i=1}^L g(i, 0)$	38.02(14)	10.228(19)	5.874(11)
	$\langle C \rangle_{SC}$	38.02(14)	10.234(19)	5.872(11)
	$\langle C ^2 \rangle_{SW} / \langle C \rangle_{SW}$	38.02(14)	10.228(19)	5.874(11)
$2L \times L$	$\frac{q}{q-1} \sum_{i=1}^{2L} g(i, 0)$	38.075(80)	10.2330(94)	5.8813(60)
	$\langle C \rangle_{SC}$	38.094(80)	10.2331(91)	5.8808(59)
	$\langle C ^2 \rangle_{SW} / \langle C \rangle_{SW}$	38.075(80)	10.2330(94)	5.8813(60)

Table 4: Numerical estimates of the correlation length $\xi_d(\beta_t)$ from four-parameter fits to the Ansatz (11) in the range $x_{\min} \dots x_{\max} = L/2$. For the $2L \times L$ lattices the fits along the x and y direction are distinguished by the index.

Lattice	$q = 10$ $L = 150$		$q = 15$ $L = 60$		$q = 20$ $L = 40$	
	x_{\min}	ξ_d	x_{\min}	ξ_d	x_{\min}	ξ_d
$L \times L$	11	8.8(3)	5	3.60(10)	3	2.21(6)
	16	8.9(4)	7	3.67(13)	4	2.21(7)
	20	9.0(5)	9	3.70(16)	5	2.24(6)
$(2L \times L)_x$	11	9.0(4)	5	3.52(5)	3	2.21(3)
	16	9.5(6)	7	3.54(7)	4	2.23(4)
	20	10.2(9)	9	3.59(10)	5	2.23(5)
$(2L \times L)_y$	11	8.9(4)	5	3.52(8)	3	2.26(4)
	16	9.1(5)	7	3.58(11)	4	2.30(6)
	20	9.3(7)	9	3.62(16)	5	2.33(7)
exact	10.559519...		4.180954...		2.695502...	

Figure Headings

Fig. 1: Integrated autocorrelation times of $g(x)$ for $q = 20$.

Fig. 2: Semi-log plots of the correlation functions $g(x)$ vs distance x on $L \times L$ and $2L \times L$ lattices for (a) $q = 10$, (b) $q = 15$, and (c) $q = 20$. The solid and dotted lines are three-parameter fits to the Ansatz (11) with ξ_d held fixed at its theoretical value. The short and long dashed lines show unconstrained four-parameter fits over the same x range. For clarity some data points are discarded.

Fig. 3: (a) Results for ξ_d of the various fits for $q = 10$ using all data points with $x_{\min} \leq x \leq x_{\max} = L/2$ as a function of x_{\min} .
(b) The effective correlation length (12) vs distance for $q = 10$. The dashed lines are constrained three-parameter fits to the data and the horizontal line shows the theoretically expected result for ξ_d .

Fig. 4 Semi-log plot of the correlation function $g(x)$ of the 2D Ising model at $\beta = 0.71 \approx 0.80\beta_c$. The two curves are fits to the Ansatz (10) with $\xi_d = 2.7232(35)$ ($L \times L$) and $\xi_d = 2.7275(24)$ ($2L \times L$), in excellent agreement with the exact result $\xi_d^{\text{theory}} = 2.728865\dots$

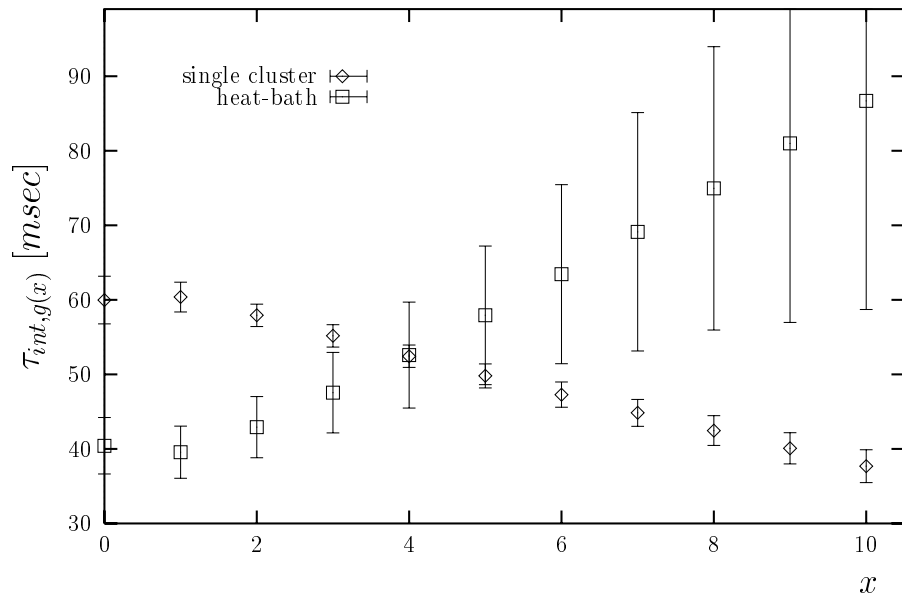


Figure 1: Integrated autocorrelation times of $g(x)$ for $q = 20$.

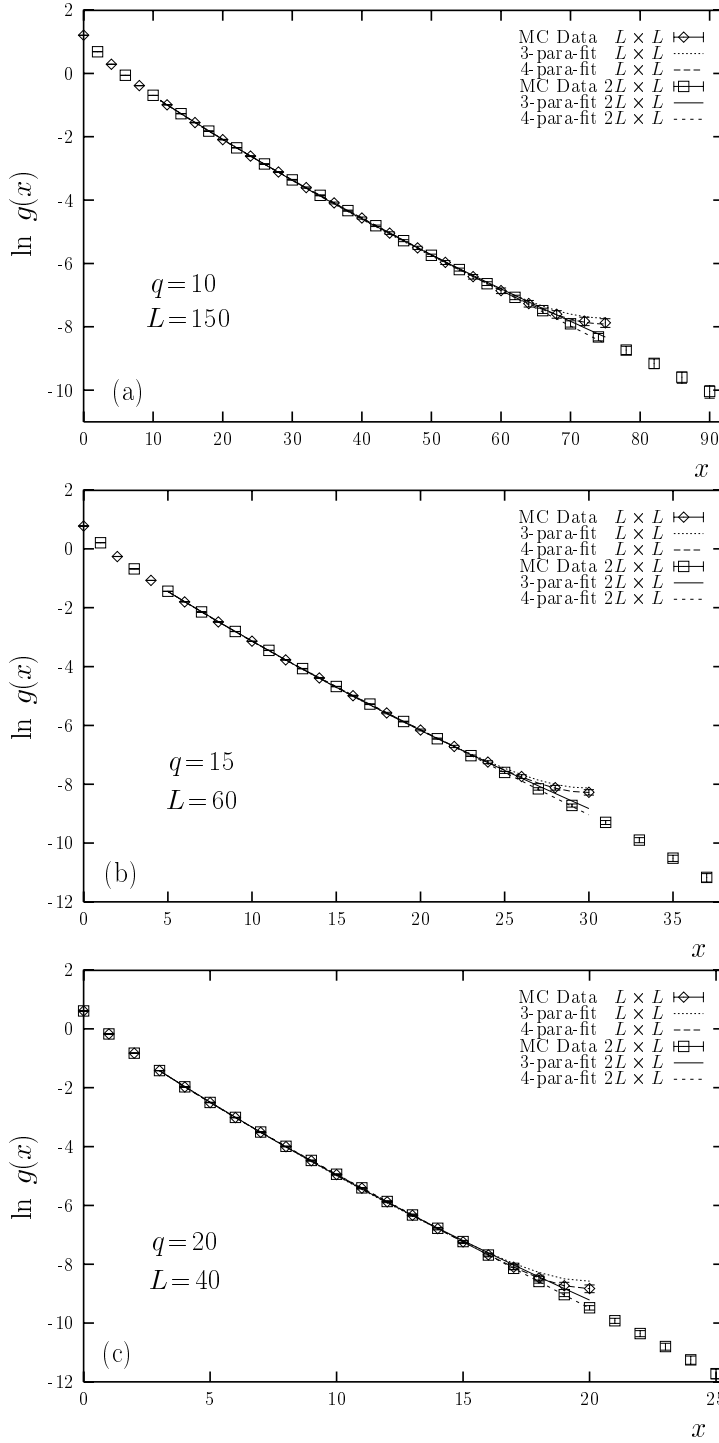


Figure 2: Semi-log plots of the correlation functions $g(x)$ vs distance x on $L \times L$ and $2L \times L$ lattices for (a) $q = 10$, (b) $q = 15$, and (c) $q = 20$. The solid and dotted lines are three-parameter fits to the Ansatz (11) with ξ_d held fixed at its theoretical value. The short and long dashed lines show unconstrained four-parameter fits over the same x range. For clarity some data points are discarded.

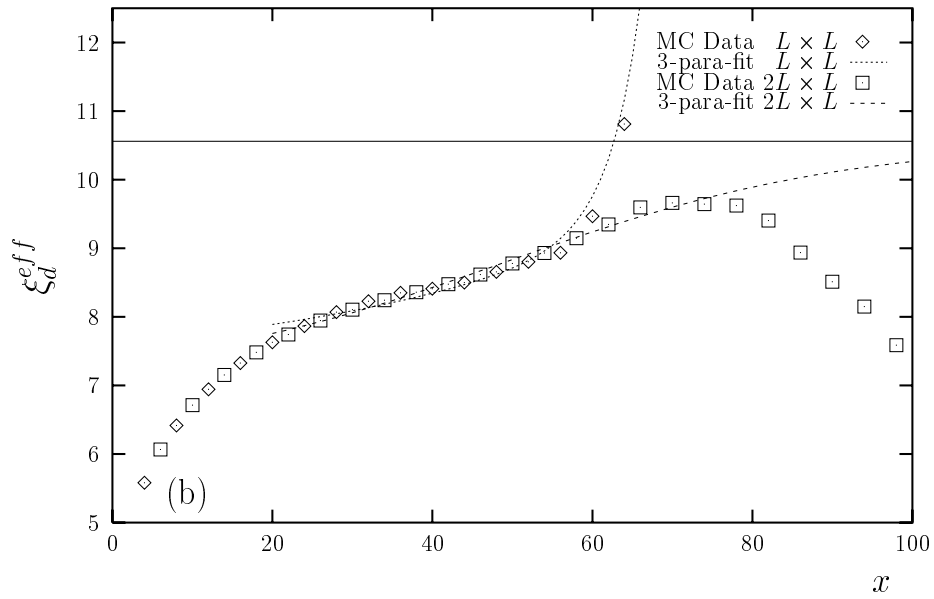
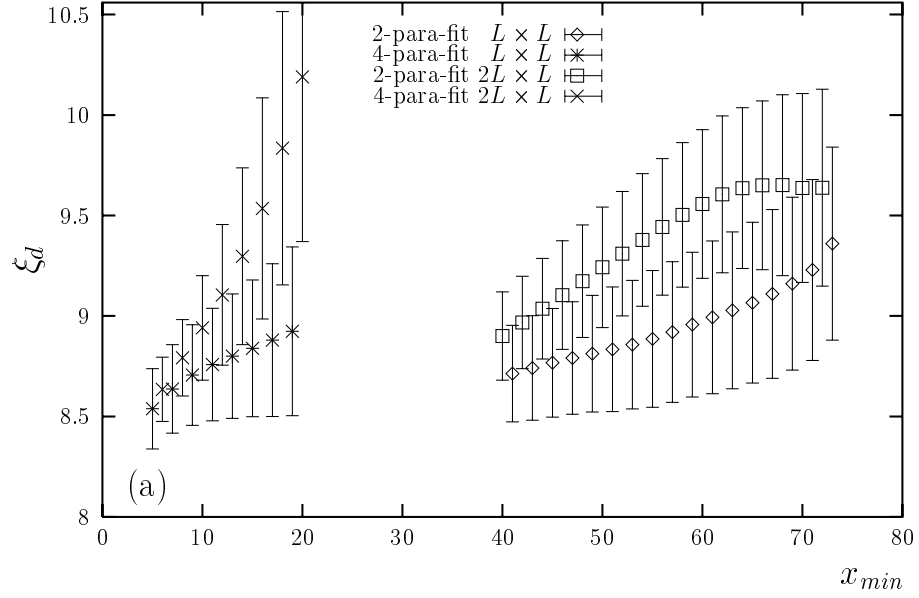


Figure 3: (a) Results for ξ_d of the various fits for $q = 10$ using all data points with $x_{min} \leq x \leq x_{max} = L/2$ as a function of x_{min} . (b) The effective correlation length (12) vs distance for $q = 10$. The dashed lines are constrained three-parameter fits to the data and the horizontal line shows the theoretically expected result for ξ_d .

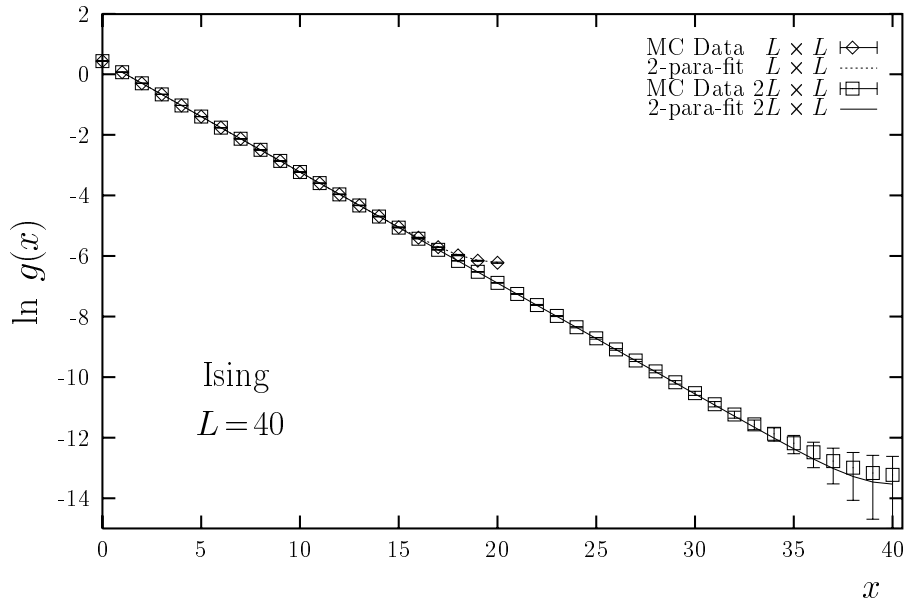


Figure 4: Semi-log plot of the correlation function $g(x)$ of the 2D Ising model at $\beta = 0.71 \approx 0.80\beta_c$. The two curves are fits to the Ansatz (10) with $\xi_d = 2.7232(35)$ ($L \times L$) and $\xi_d = 2.7275(24)$ ($2L \times L$), in excellent agreement with the exact result $\xi_d^{\text{theory}} = 2.728865\dots$